The roles of autophagy in the treatment of diabetic nephropathy with rapamycin

Ya Fu[A–F], Liang Zhang[A–F], Shupei Qin[A,B,E,F], Meng Tang[A], Yanxia Hao[A], Xuedong Chen[B,C], Yan Wang[A], Ting Zhou[A], Yuemei Xue[A], Long Cheng[A], Na Liu[A], Qifeng Jia[A], Yangyang Chen[A], Li Li[A]

Department of Nephrology, Ordos Central Hospital, Inner Mongolia Medical University, China

A – research concept and design; B – collection and/or assembly of data; C – data analysis and interpretation; D – writing the article; E – critical revision of the article; F – final approval of the article

Advances in Clinical and Experimental Medicine, ISSN 1899–5276 (print), ISSN 2451–2680 (online) *Adv Clin Exp Med*. 2024;33(10):1141–1152

Address for correspondence
Ya Fu
E-mail: fuya01200418@163.com

Funding sources
The study was supported by the Inner Mongolia Natural Science Foundation in China (grant No. 2020MS08089).

Conflict of interest
None declared

Received on November 19, 2022
Reviewed on May 25, 2023
Accepted on November 23, 2023

Published online on February 6, 2024

Abstract

Background. Rapamycin is known to induce autophagy, promote cell survival and inhibit the progression of diabetic nephropathy (DN).

Objectives. The aim of this study was to examine the role of autophagy in the treatment of DN with rapamycin to provide the basis for the DN treatment with rapamycin.

Materials and methods. Human mesangial cells (HMC) were cultured in a constant temperature incubator with 5% CO_2, at 37°C and saturated humidity. Cells were divided into 5 groups and the 5-ethynyl-2-deoxyuridine (EdU) cell proliferation assay was used to determine cell proliferation. Flow cytometry was used to determine cell apoptosis, while GFP–RFP–LC3 showed autophagy flow. Western blot was employed to detect the expression of autophagy-related proteins LC3-II/LC3-I and P62. Enzyme-linked immunosorbent assay (ELISA) was used to determine the contents of type IV collagen fiber (Col4), hyaluronic acid (HA) and laminin (LA) in the extracellular matrix (ECM).

Results. Cell proliferation was the lowest in the hyperglycemic group. Additionally, the hyperglycemic group displayed the lowest number of autolysosomes compared to other groups. In contrast, the rapamycin group exhibited the highest number of autolysosomes. The LC3-II/LC3-I ratio was also the lowest in the hyperglycemic group, measuring 0.53 (0.50–0.58), while the expression level of P62 was significantly higher in that group at 0.98 (0.95–1.01) compared to other groups. Upon the introduction of rapamycin, the LC3-II/LC3-I ratio was significantly increased at 2.21 (1.95–2.21), and P62 was significantly decreased 0.38 (0.38–0.39) compared to the hyperglycemic group. Both changes were statistically significant, with p-values of 0.034 and 0.010, respectively. Enzyme-linked immunosorbent assay was employed to detect Col4, HA and LA content. The study findings demonstrated significantly higher levels of glucose in the hyperglycemic group in comparison to other groups. In contrast, the rapamycin group exhibited significantly lower levels of glucose than the hyperglycemic group, yet the difference was not statistically significant.

Conclusions. Hyperglycemic can inhibit the autophagic activity of HMC, promote cell apoptosis, enhance ECM accumulation, and facilitate the DN progression. In contrast, rapamycin can elicit autophagy, decrease mesangial matrix proliferation, and therefore impede DN progression.

Key words: diabetic nephropathy, autophagy, human mesangial cells

Cite as
Fu Y, Zhang L, Qin S, et al. The roles of autophagy in the treatment of diabetic nephropathy with rapamycin. *Adv Clin Exp Med*. 2024;33(10):1141–1152. doi:10.17219/acem/175776

DOI
10.17219/acem/175776

Background

At present, diabetic nephropathy (DN) has become the leading cause of end-stage renal disease (ESRD) in China. The treatment of DN is difficult, and there is no recognized specific drug that can cure DN. It is an urgent problem to further understand the pathogenesis of DN and seek effective treatment. Mesangial cells are extremely important target cells and effector cells in the development of DN, participating in the process of glomerular injury and repair, and promoting inflammation and the development of glomerular sclerosis together with extracellular matrix (ECM). At the same time, oxidative stress, inflammation and autophagy are also involved in various pathological processes of DN.

Autophagy refers to the formation of autophagosomes in the cytoplasm to degrade damaged organelles, proteins and other components to meet the metabolic needs of the cells themselves and help the cells survive. According to the different forms, autophagy can be divided into macroautophagy, microautophagy and chaperone-mediated autophagy, among which macroautophagy is the most common. Autophagy is a continuous dynamic process that involves 5 distinct stages: initiation, nucleation, expansion and elongation, closure and fusion, and cargo degradation The autophagy process is regulated by several autophagy-related genes (ATG). Autophagy is activated under stress, such as hypoxia, amino acid deficiency or low glucose, and forms autophagosomes after activation to remove damaged cell components and ensure cell survival. It is the process of fusing macromolecular proteins, mitochondria, ribosomes, and organelle fragments with autophagosomes to break them down into small molecules.[1]

Autophagy and proteasome pathways belong to 2 intracellular degradation pathways, but the contents degraded by the 2 are different. The latter specifically degrades ubiquitinated small protein molecules, while the denatured, misfolded large protein molecules and aging and deteriorated organelles are degraded by autophagy. Therefore, cells generally maintain some level of autophagy activity, and the level of autophagy varies depending on the tissue type. Under the condition of hyperglycemia, autophagy activity of mesangial cells is inhibited, but with the increase of intracellular advanced glycation end products (AGEs), a large number of proteins are inactivated, and organelle function is impaired. At this point, both protein degradation pathways may be activated. Although autophagy changes at different stages of DN are still a controversial issue, most evidence supports the fact that the process of renal autophagy is blocked in DN, promoting apoptosis and the occurrence of disease. As an inducer of autophagy, rapamycin enables cells to survive and resist external damage.

This study will further verify the autophagy of cells under the condition of high glucose, whether high glucose has an effect on cell survival, and the effect of rapamycin on the autophagy activity of cells, providing evidence for the application of rapamycin in diabetic nephropathy.

Objectives

To study the role of autophagy in the treatment of DM with rapamycin and to provide the basis for the treatment of DN with rapamycin.

Materials and methods

Materials

Human mesangial cells (HMC) were purchased from the Shanghai Fuheng Biology (Shanghai, China; cat. No. FH0241) and cell culture flasks were purchased from FALCON (Chongqing, China; cat. No. 353014).

Culture and grouping of mesangial cells

Human mesangial cells were cultured in Dulbecco's modified Eagle's medium (DMEM) containing 10% fetal bovine serum (FBS), 100 U/mL penicillin and 100 U/mL streptomycin in a constant temperature incubator with 5% CO_2, at 37°C and saturated humidity. The HMC group was cultured in the original medium component without glucose. The hypoglycemic group was cultured in medium containing 5 mmol/L glucose. In the hyperglycemic group, HMCs were cultured in medium containing 30 mmol/L glucose. In isotonic mannitol group HMCs were cultured in medium containing 24.5 mmol/L mannitol and 5.5 mmol/L glucose. In the rapamycin group, HMCs were cultured in the medium containing 30 mmol/L glucose and 1 μM rapamycin.

Proliferation of 5-ethynyl-2-deoxyuridine (EdU) cells

The cells were treated with 2 × EdU working solution for 2 h, fixed with 4% paraformaldehyde and incubated for 30 min. The cells were cultured using conventional methods. After discarding the fixed solution in the culture medium, the cells were washed 3 times and incubated with a transparent solution at room temperature for 20 min. Following this, the cells were incubated at room temperature away from light for 30 min before being observed under a fluorescence microscope (Olympus IX71; Olympus Corp., Tokyo, Japan).

Apoptosis cells were determined with flow cytometry

After digesting the HMC with trypsin, they were collected by centrifugation at 2,000 rpm for 5–10 min and then washed again. Following this, 300 µL of buffer suspension cells were added, and 5 µL of Annexin V-FITC was mixed in. The resulting mixture was kept away from light. Before loading the sample, 5 µL of propidium iodide (PI) staining was added and allowed to bind for 5 min. Finally, after adding 200 µL of buffer, the results were observed.

GFP–RFP–LC3 labeling autophagy flow

The HMC were inoculated into 24-well plates, The amount of GFP–RFP–LC3 adenovirus in each group was within the range of multiplicity of infection (MOI) = 20. After 2 h, the medium was changed, and the cells were washed with culture medium or buffer. After the cleaning solution was carefully absorbed, the cells were fixed with a freshly prepared and pre-heated buffer containing 4% paraformaldehyde for 10 min at room temperature. The fixative was removed, and the cells were rinsed several times with an appropriate buffer. Nuclear staining was performed in a dark room to avoid light. Fluorescent dye was applied diluted (DAPI (4',6-diamidino-2-phenylindole, 1:1,000)), washed cells were applied and incubate at room temperature for 7–10 min, and then wash 3 times for 5 min with phosphate-buffered saline (PBS); finally, the liquid was discarded. The film was sealed and observed with a confocal laser microscope (Leica TCS SP8; Leica Camera AG, Wetzlar, Germany).

Protein concentrations of LC3-II/LC3-I and P62 were detected with western blot

Cell pellets from each group were collected. A total of 150 µL of lysate was added to each sample, and gel plates were prepared in the following manner: 1. The polyvinylidene fluoride (PVDF) membrane was sealed with a sealing solution containing 5% skim milk powder at room temperature for 2 h. 2. The corresponding primary antibody (rabbit anti-human LC3, P62) was diluted with blocking solution. The PVDF membrane was then immersed in the primary antibody incubation solution and incubated overnight at 4°C. 3. Excess primary antibodies were removed by washing the PVDF membrane thoroughly in Tris-buffered saline with Tween (TBST) and repeating the process 3–4 times for 15 min each time. 4. The secondary antibody was applied (goat anti-rabbit IgG antibody) and the PVDF membrane was soaked in the solution for secondary antibody incubation and incubated at 37°C for 2 h. 5. Excess secondary antibodies were washed away by fully washing the PVDF membrane in TBST 3–4 times for 15 min each time. 6. Color exposure was performed.

The content of Col4 HA, and LA of cells was determined by ELISA

Cells digested with trypsin were harvested and the resulting supernatant was collected. Biotinylated antibody working solution (100 µL) was added to each well, followed by incubation at 37°C for 1 h after covering the plate with film. Enzyme conjugate working solution (100 µL) was then added to each well, followed by substrate (tetramethylbenzidine) solution (90 µL). The enzyme plate was covered with film and incubated away from light. Stop solution (50 µL) was added to each well and the optical density (OD) was immediately measured at 450 nm using a microplate reader (Multiskan Mk3 Microplate Reader; Thermo Fisher Scientific, Waltham, USA).

Statistical analyses

IBM SPSS v. 26.0 (IBM Corp., Armonk, USA) software was utilized for statistical analysis. The experimental data were replicated 3 times for each group. All tested variables were expressed as medians with interquartile ranges (IQRs; 25^{th} to 75^{th} percentiles). We assessed statistical differences with the Kruskal–Wallis test, followed by Dunn's test for multiple comparisons. We adjusted p-values using the Bonferroni correction. We considered a p-value below 0.05 statistically significant. Bootstrap medians and 95% confidence intervals (95% CIs) have been reported.

Results

EdU cell proliferation under different conditions

Hoechst 33342 stimulated the nuclei to emit blue fluorescence, while Azide 488 caused proliferation of cells resulting in green fluorescence. Figure 1 shows a significant number of cells in HMC group, hypoglycemic group and isotonic mannitol group, which were 948.5 (881.75–1008.5), 1019.5 (938.5–1055.5) and 920.5 (808.5–954.5), respectively. Additionally, there were a considerable number of proliferating cells: 463.0 (416.75–514.5), 512.5 (462.25–525.25 and 444.5 (411.75–513.25) were the measured values for total number of cells in hyperglycemic group. The group contained 912.0 (860.5–969.5) cells in total. Among them, only 141.0 (130.0–163.25) were found to be proliferating. The proliferation rate of cells in hyperglycemic group was statistically significant compared to HMC group (p-value 0.017), with a rate of 17.5% (13.75–19.75%). Table 1 displays the results, while Table 2 and Table 3 show the nonparametric test results and post hoc analysis, respectively. Hoechst 33342 induced blue fluorescence in all nuclei, while Azide 488 induced green fluorescence in proliferating cells. Figure 1A,B,D illustrates a significant number of cells: 948.5 (881.75–1008.5), 1019.5 (938.5–1055.5)

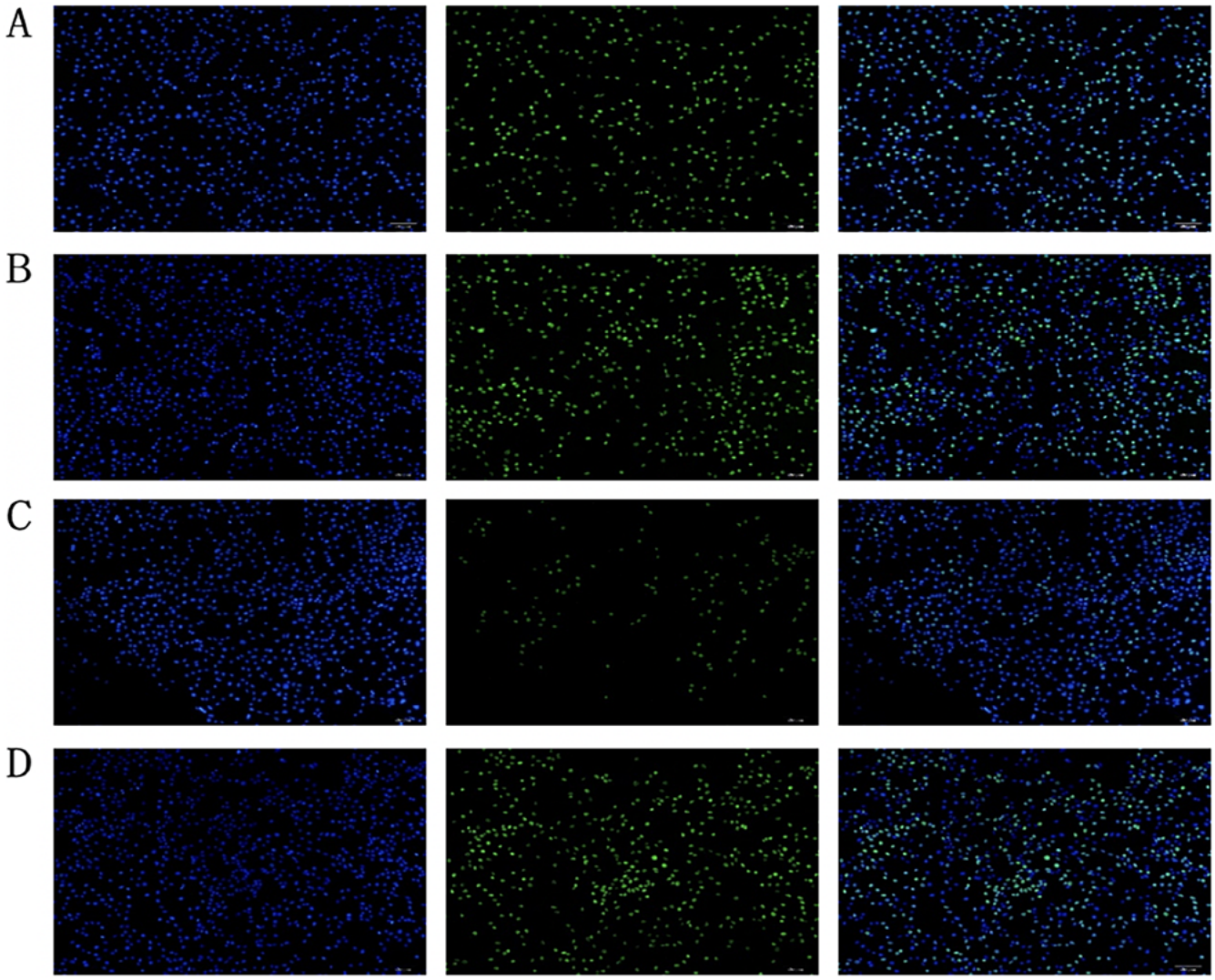

Fig. 1. Proliferation of 5-ethynyl-2-deoxyuridine (EdU) cells under fluorescence microscope. A. Human mesangial cells (HMC); B. Hypoglycemic group; C. Hyperglycemic group; D. Mannitol isotonic group. The blue fluorescence represents nucleated cells and the green fluorescence represents proliferating cells. The number of cells in group C was 912 (860.5–969.5), and in groups A, B and D it was 948.5 (881.75–1008.5), 1019.5 (938.5–1055.5) and 920.5 (808.5–954.5), respectively. The cell proliferation rate of group C was 17.5% (13.75–19.75%), which was statistically significant compared with group A (p-value at 0.017)

and 920.5 (808.5–954.5), respectively. Furthermore, there was a considerable number of proliferating cells: the total cell count for hyperglycemic group was 912.0 (860.5–969.5) and the number of proliferating cells was 141.0 (130.0–163.25). The proliferation rate of cells in group C was 17.5% (13.75–19.75%), indicating significant statistical difference from HMC group with a p-value of 0.017.

Flow cytometry detection of cell apoptosis

Flow cytometry was utilized to evaluate cell apoptosis in various conditions, as depicted in Fig. 2. The proportion of apoptotic cells in HMC group, hypoglycemic group and isotonic mannitol group were 2.6% (2.52–2.65%), 3.86% (3.77–3.87%) and 3.41% (3.37–3.53%), respectively, based on the data presented in Table 4. Notably, these rates were significantly lower than the 16.04% (16.03–16.55%) proportion in hyperglycemic group. The survival rates of cells in HMC group, hypoglycemic group and isotonic mannitol group were 93.0% (92.75–93.55%), 93.2% (92.4–93.25%) and 93.8% (93.25–94.0%), respectively. The survival rate of cells in group C was 79.0% (78.55–79.4%). The number of apoptotic cells in hyperglycemic group was statistically significant (p-value = 0.013) compared to HMC group. The nonparametric test results and post hoc analysis are shown in Table 5 and Table 6.

GFP-RFP-LC3 dual fluorescence labeling of autophagy flow

The red fluorescent protein (RFP) emitted red fluorescence, while the green fluorescent protein (GFP) emitted green fluorescence. Yellow spots represented autophagosomes, while red spots represented autolysosomes. As shown in Fig. 3, hyperglycemic group had the lowest number of autolysosomes, while HMC group, hypoglycemic

Table 1. General statistical description of 5-ethynyl-2-deoxyuridine (EdU) cell proliferation tests

Group	Median (25–75% quartile)	Lower 95% CI	Upper 95% CI
Number of proliferating cells			
HMC	463 (514.5–416.75)	399	523.38
Hypoglycemic group	512.5 (525.25–462.25)	399	618.5
Hyperglycemic group	141 (163.25–130)	113	156.433
Mannitol isotonic group	444.5 (513.25–411.75)	348.175	529.5
Total number of cells			
HMC	948.5 (1008.5–881.75)	831	1089.528
Hypoglycemic group	1019.5 (1055.5–938.5)	908.5	1199
Hyperglycemic group	912 (969.5–860.5)	828	1047.5
Mannitol isotonic group	920.5 (954.5–808.5)	862.5	1129.151
Proliferation rate			
HMC	50.5 (53.5–47.5)	45.027	57.5
Hypoglycemic group	50 (51.75–48.25)	47	54
Hyperglycemic group	17.5 (19.75–13.75)	15	22
Mannitol isotonic group	51.5 (53–47)	48.5	58

All tested variables were expressed as medians with interquartile ranges (IQRs) (25^{th}–75^{th} percentiles). Bootstrap medians 95% confidence intervals (95% CIs) were reported in the table; EdU – 5-ethynyl-2-deoxyuridine; HMC – human mesangial cells.

Table 2. Nonparametric test results of 5-ethynyl-2-deoxyuridine (EdU) cell proliferation tests

Variables	Statistics	p-value	df
Number of proliferating cells	13.253	0.004	3
Total number cells	3.427	0.330	3
Proliferation rate	13.059	0.005	3

The Kruskal–Wallis test was used. The significance level of the mean difference was 0.05.

group and isotonic mannitol group had more autolysosomes than hyperglycemic group, with rapamycin group having the highest number of autolysosomes.

Expression levels of autophagy markers LC3 and P62 were detected with western blotting

The results indicate that in hyperglycemic group, there was a significant increase in the expression of P62 and an apparent decrease in the expression of autophagy marker LC3-II, while the expression of LC3-I was apparently increased, as compared to HMC group, hypoglycemic group and isotonic mannitol group. These results are presented in Fig. 4 and Fig. 5. When rapamycin was added to the sample (rapamycin group), the expression level of LC3-II increased significantly, while the expression levels of LC3-I and P62 decreased significantly. The LC3-II/LC3-I ratio was 2.21 (1.95–2.21), which was significantly higher than that of the other groups. Also, the expression

Table 3. The multiple comparison of post hoc analysis of 5-ethynyl-2-deoxyuridine (EdU) cell proliferation tests

Variables	Comparison	Statistics	p-value	p-value adjustment
Number of proliferating cells	A–B	– 0.470	0.639	1
	A–C	2.777	0.005	0.033
	B–C	3.247	0.001	0.007
	A–D	– 0.020	0.984	1
	B–D	0.449	0.653	1
	C–D	– 2.798	0.005	0.031
Total number cells	A–B	– 0.898	0.369	1
	A–C	0.653	0.514	1
	B–C	1.551	0.121	0.725
	A–D	0.735	0.462	1
	B–D	1.633	0.102	0.615
	C–D	0.082	0.935	1
Proliferation	A–B	0.184	0.854	1
	A–C	2.984	0.003	0.017
	B–C	2.800	0.005	0.031
	A–D	– 0.061	0.951	1
	B–D	–0.245	0.806	1
	C–D	–3.045	0.002	0.014

Multiple comparisons were detected with Dunn's test and p-values were adjusted using the Bonferroni correction; A – HMC (human mesangial cells); B – hypoglycemic group; C – hyperglycemic group; D – mannitol isotonic group; the significance level of the mean difference was 0.05.

Table 4. General statistical description of cell apoptosis under different conditions was detected using flow cytometry

Groups	Median (25–75% quartile)	Lower 95% CI	Upper 95% CI
Q2 + Q3			
HMC	2.6 (2.515–2.645)	2.51	2.77
Hypoglycemia group	3.86 (3.77–3.87)	3.84	4.04
Hyperglycemia group	16.04 (16.03–16.55)	15.02	16.06
Mannitol isotonic group	3.41 (3.37–3.525)	3.18	3.49
Q4			
HMC	93 (92.75–93.55)	91.9	93.5
Hypoglycemia group	93.2 (92.4–93.25)	93.1	94.8
Hyperglycemia group	79 (78.55–79.4)	78.2	79.9
Mannitol isotonic group	93.8 (93.25–94)	93.4	94.9

All tested variables were expressed as medians with interquartile ranges (IQRs) (25^{th}–75^{th} percentiles). Bootstrap medians 95% confidence intervals (95% CI) were reported in the table; Q2 and Q3 – apoptotic cells; Q4 – living cells; HMC – human mesangial cells.

level of P62 was 0.38 (0.375–0.39), which was significantly lower than that of the other groups. The levels of P62 expression and the ration of LC3-II/LC3-I in hyperglycemic group significantly differed from those in rapamycin group, with p-values of 0.01 and 0.03, respectively, as displayed in Table 7. Table 8 and Table 9 illustrate the nonparametric test results and post hoc analysis.

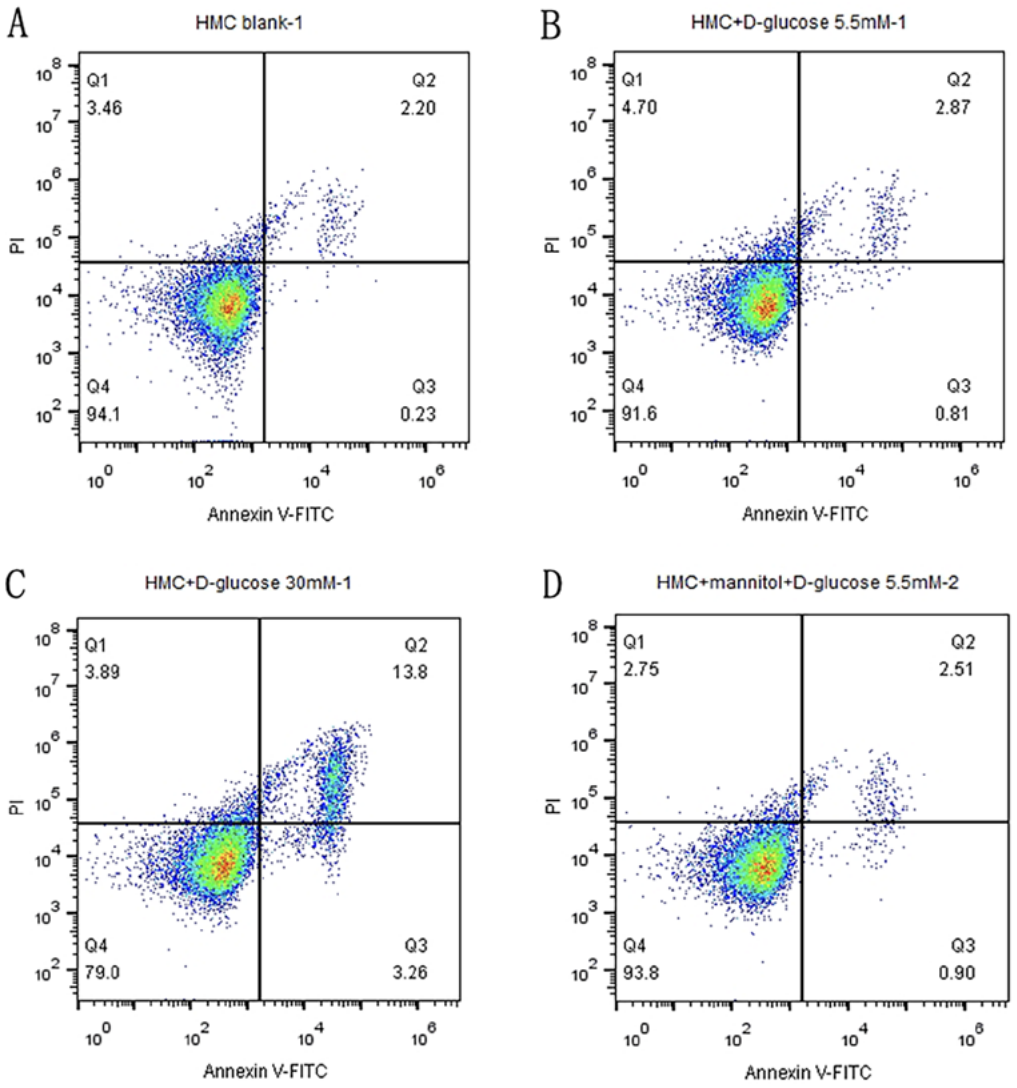

Fig. 2. Cell apoptosis under different conditions was detected with flow cytometry. A. Human mesangial cells (HMC); B. Hypoglycemic group; C. Hyperglycemic group; D. Mannitol isotonic group; Q1 – cell debris; Q2 and Q3 – apoptotic cells; Q4 – living cells. The proportion of apoptotic cells in groups A, B and D were 2.6% (2.52–2.65%), 3.86% (3.77–3.87%) and 3.41% (3.37–3.53%), respectively, which was significantly lower than that in group C: 16.04% (16.03–16.55%). The survival rates of cells in group C was the lowest and amounted to 79.0% (78.55–79.4%). Compared with group A, the number of apoptotic cells in group C was statistically significant (p = 0.013)

Table 5. Nonparametric test results of apoptosis test

Variables	Statistics	p-value	df
Q2	8.929	0.030	3
Q3	9.462	0.024	3
Q4	6.897	0.075	3
Q2 + Q3	10.385	0.016	3

The Kruskal–Wallis test was used. df – degrees of freedom; Q2 and Q3 – apoptotic cells; Q4 – living cells; the significance level of the mean difference was 0.05.

Table 6. Multiple comparison of apoptotic cells post hoc analysis

Variables	Comparison	Statistic	p-value	p-value adjustment
Q4	A–B	0.226	0.821	1
	A–C	1.925	0.054	0.325
	B–C	1.698	0.089	0.537
	A–D	–0.566	0.571	1
	B–D	–0.793	0.428	1
	C–D	–2.491	0.013	0.076
Q2 + Q3	A–B	–2.038	0.042	0.249
	A–C	–3.057	0.002	0.013
	B–C	–1.019	0.308	1
	A–D	–1.019	0.308	1
	B–D	1.019	0.308	1
	C–D	2.038	0.042	0.249

Multiple comparisons were detected with Dunn's test and p-values were adjusted using the Bonferroni correction; A – HMC (human mesangial cells); B – hypoglycemic group; C – hyperglycemic group; D – mannitol isotonic group; Q2 and Q3 – apoptotic cells; Q4 – living cells; the significance level of the mean difference was 0.05.

The contents of Col4, HA and LA in cells were detected with ELISA

The main elements of ECM were detected using ELISA and displayed in Fig. 6. In the hyperglycemic group, the levels of IV collagen fiber (Col4), hyaluronic acid (HA) and laminin (LA) were significantly higher compared to those in the HMC, hypoglycemic and mannitol isotonic groups. The levels were as follows: 18.65 (17.04–19.43) ng/mL, 89.17

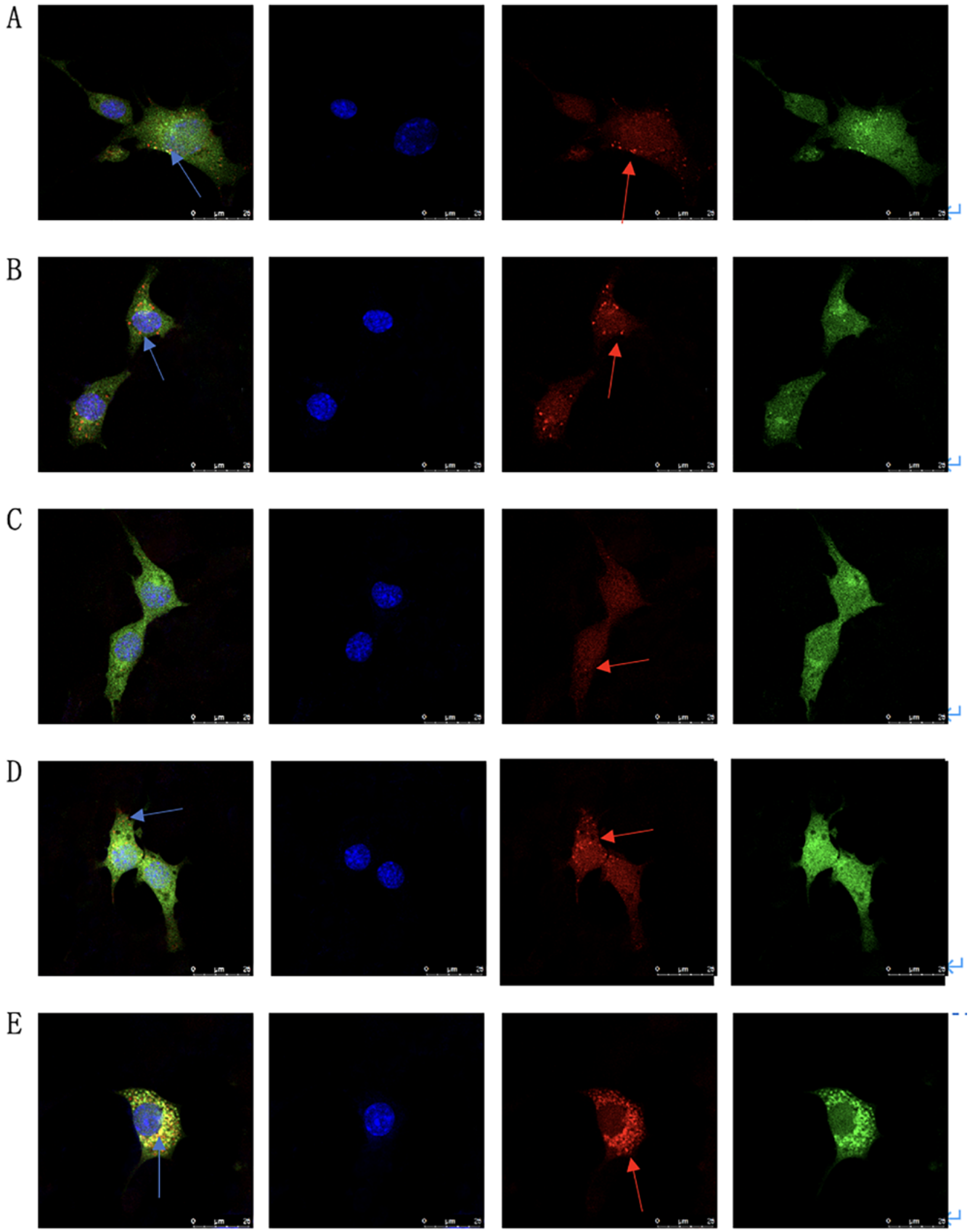

Fig. 3. GFP-RFP-LC3 labeled autophagy flow. A. Human mesangial cells (HMC); B. Hypoglycemic group; C. Hyperglycemic group; D. Mannitol isotonic group; E. Rapamycin group. Yellow spots represent autophagosomes and red spots represent autolysosomes. Group C had the least number of autolysosomes, while groups A, B, D and E had more autolysosomes than group C, among which group E had the most autolysosomes

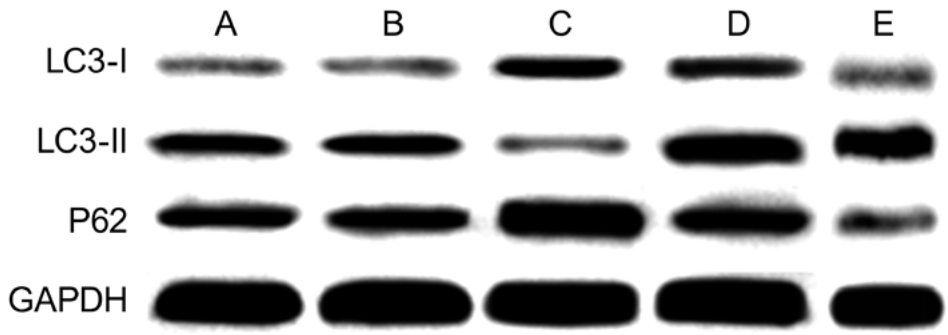

Fig. 4. The expression levels of LC3-II, LC3-I and P62 in mesangial cells were detected with western blotting; A – human mesangial cells (HMC); B – hypoglycemic group; C – hyperglycemic group; D – mannitol isotonic group; E – rapamycin group; GAPDH – control group. In group C, the expression of autophagy marker LC3 was the lowest, while the expression of LC3-I and P62 was the highest, but they had no difference in groups A, B, D, and E.

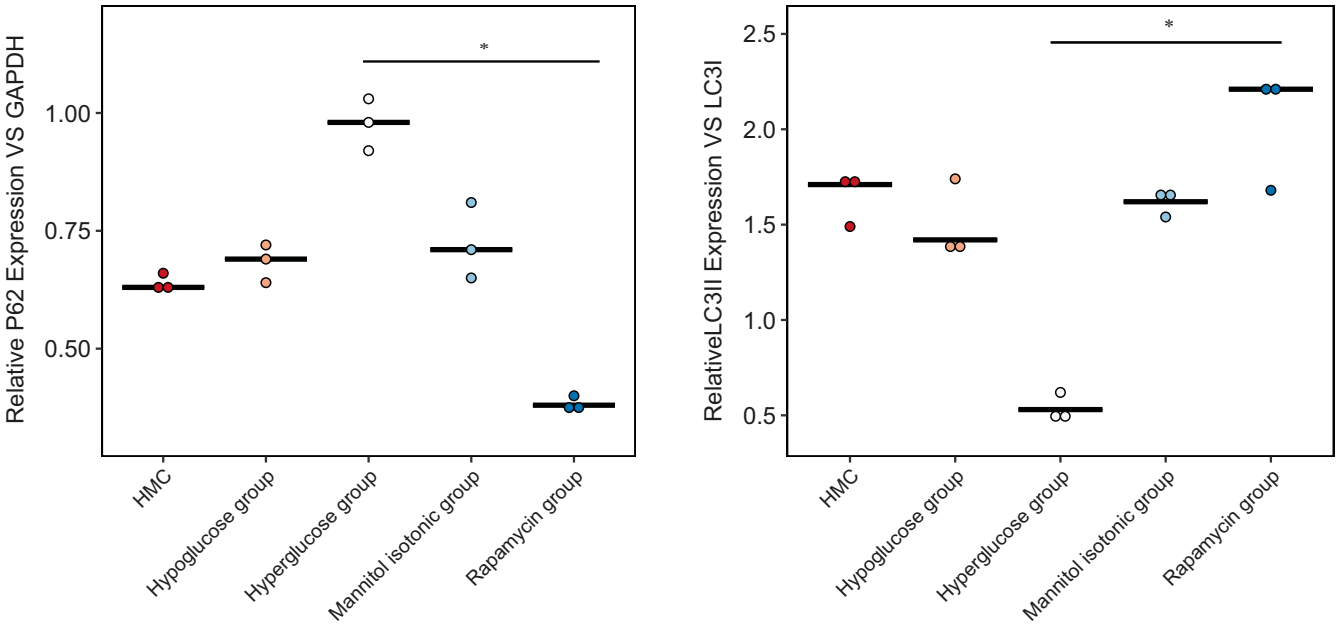

Fig. 5. Expression levels of LC3-II/LC3-I ratio and P62 in cells were detected with western blotting. Point means the raw data values and black lines mean median of each group. The Kruskal–Wallis test was applied to test differences between 5 compared group. Multiple comparisons were detected with Dunn's test and p-values were adjusted using the Bonferroni correction. In the hyperglycemic group, the LC3-II/LC3-I ratio was lower, P62 was increased, but in the rapamycin group, the expression of LC3-II/LC3-I ratio and P62 was different compared to hyperglycemic group

*hyperglycemic group was significantly different from rapamycin group; p-values of 0.03 and 0.01, respectively.

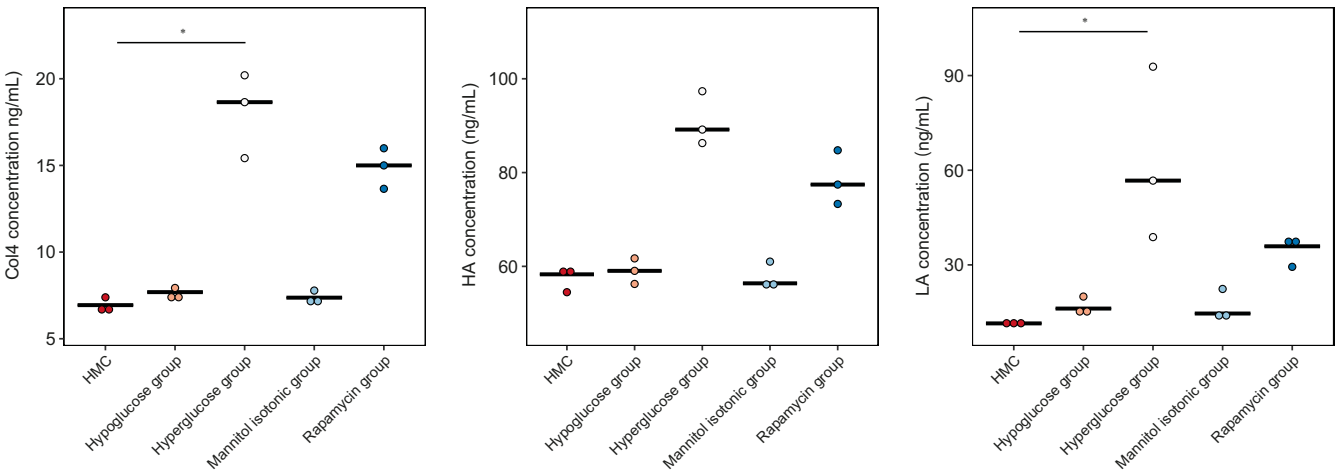

Fig. 6. The levels of type IV collagen fiber (Col4), hyaluronic acid (HA) and laminin (LA) in cells were detected with enzyme-linked immunosorbent assay (ELISA). Points mean the raw data values and black lines mean median of each group. The Kruskal–Wallis test was used to test differences between 5 compared group. Multiple comparisons were detected with Dunn's test, and p-values were adjusted using Bonferroni correction

* human mesangial cells (HMC) group was significantly different from hyperglycemic group.

Table 7. General statistical description of western blotting detection of p62 and LC3-II/LC3-I

Group	P62			LC3-II/LC3-I		
	median (25–75% quartile)	lower 95% CI	upper 95% CI	median (25–75% quartile)	lower 95% CI	upper 95% CI
HMC	0.63 (0.645–0.63)	0.6	0.63	1.71 (1.725–1.6)	1.68	1.93
Hypoglycemic group	0.69 (0.705–0.665)	0.66	0.74	1.42 (1.58–1.385)	1.1	1.49
Hyperglycemic group	0.98 (1.005–0.95)	0.93	1.04	0.53 (0.575–0.495)	0.44	0.6
Mannitol isotonic group	0.71 (0.76–0.68)	0.61	0.77	1.62 (1.655–1.58)	1.55	1.7
Rapamycin group	0.38 (0.39–0.375)	0.36	0.39	2.21 (2.21–1.945)	2.21	2.74

All tested variables were expressed as medians with interquartile ranges (IQRs) (25^{th}–75^{th} percentiles). Bootstrap medians 95% confidence intervals (95% CIs) were reported in the table. HMC – human mesangial cells.

Table 8. Nonparametric test results of LC3-II/LC3-I and P62 in western blotting detection

Variables	Statistics	p-value	df
P62	12.122	0.016	4
LC3	9.325	0.053	4

The Kruskal–Wallis test was used. The significance level of the mean difference was 0.05; df – degrees of freedom.

Table. 9. Expression levels of LC3-II/LC3-I and P62 in western blotting multiple comparisons post hoc analysis

Variables	Comparison	Statistics	p-value	p-value adjustment
P62	A–B	–0.822	0.411	1
	A–C	–2.284	0.022	0.224
	B–C	–1.462	0.144	1
	A–D	–1.096	0.273	1
	B–D	–0.274	0.784	1
	C–D	1.188	0.235	1
	A–E	1.005	0.315	1
	B–E	1.827	0.068	0.676
	C–E	3.289	0.001	0.010
	D–E	2.101	0.036	0.356
LC3-II/LC3-I	A–B	0.732	0.464	1
	A–C	2.149	0.032	0.316
	B–C	1.417	0.156	1
	A–D	0.412	0.681	1
	B–D	–0.320	0.749	1
	C–D	–1.736	0.082	0.823
	A–E	–0.777	0.437	1
	B–E	–1.509	0.131	1
	C–E	–2.926	0.003	0.034
	D–E	–1.189	0.234	1

Multiple comparisons were detected with Dunn's test and p-values were adjusted using the Bonferroni correction; A – HMC (human mesangial cells); B – hypoglycemic group; C – hyperglycemic group; D – mannitol isotonic group; E – rapamycin group. The significance level of the mean difference was 0.05.

Table 10. Type IV collagen fiber (Col4), hyaluronic acid (HA) and laminin (LA) contents of cells in different states were detected using enzyme-linked immunosorbent assay (ELISA)

Group	Median (25–75% quartile)	Lower 95% CI	Upper 95% CI
Col4			
HMC	6.94 (7.165–6.69)	6.49	7.44
Hypoglycemic group	7.69 (7.81–7.395)	7.45	8.28
Hyperglycemic group	18.65 (19.425–17.035)	17.1	21.88
Mannitol isotonic group	7.37 (7.575–7.165)	6.96	7.78
Rapamycin group	15 (15.495–14.325)	14.01	16.35
HA			
HMC	58.3 (58.875–56.395)	57.15	62.11
Hypoglycemic group	59.04 (60.37–57.645)	56.38	61.83
Hyperglycemic group	89.17 (93.255–87.73)	81	92.05
Mannitol isotonic group	56.38 (58.695–56.15)	51.75	56.84
Rapamycin group	77.44 (81.095–75.375)	70.13	81.57
LA			
HMC	11.46 (11.83–11.14)	10.72	12.1
Hypoglycemic group	16.16 (18.06–15.225)	12.36	18.03
Hyperglycemic group	56.71 (74.76–47.76)	20.61	74.61
Mannitol isotonic group	14.59 (18.48–13.965)	6.81	15.84
Rapamycin group	35.89 (37.35–32.635)	32.97	42.4

All tested variables were expressed as medians with interquartile ranges (IQRs) (25^{th}–75^{th} percentiles). Bootstrap medians 95% confidence intervals (95% CIs) were reported in the table. HMC – human mesangial cells.

(87.73–93.23) ng/mL and 56.71 (47.76–74.76) ng/mL, respectively. Compared to the HMC group, there was a significant difference in Col4 and LA levels with p-values of 0.035 and 0.012, respectively. Upon the addition of rapamycin, the hyperglycemic group demonstrated a significant decrease in the levels of Col4, HA and LA, although no statistical significance was observed, as indicated in Table 10. The nonparametric test results and post hoc analysis are presented in Table 11 and Table 12. Under hyperglycemic conditions, the concentrations of Col4, HA and LA were significantly elevated in comparison to the other groups (represented by the hyperglycemic group as compared to HMC; $p < 0.05$). Although there was

Table 11. Nonparametric test results of type IV collagen fiber (Col4), hyaluronic acid (HA) and laminin (LA)

Variables	Statistics	p-value	df
Col4	11.567	0.021	4
HA	11.033	0.026	4
LA	12.714	0.013	4

The Kruskal–Wallis test was used. The significance level of the mean difference was 0.05; df – degrees of freedom.

Table 12. Type IV collagen fiber (Col4), hyaluronic acid (HA) and laminin (LA) multiple comparisons post hoc analysis

Variables	Comparison	Statistics	p-value	p-value adjustment
Col4	A–B	–1.004	0.315	1
	A–C	–2.921	0.003	0.035
	B–C	–1.917	0.055	0.552
	A–D	–0.639	0.523	1
	B–D	0.365	0.715	1
	C–D	2.282	0.022	0.225
	A–E	–2.282	0.022	0.225
	B–E	–1.278	0.201	1
	C–E	0.639	0.523	1
	D–E	–1.643	0.100	1
HA	A–B	–0.456	0.648	1
	A–C	–2.647	0.008	0.081
	B–C	–2.191	0.028	0.284
	A–D	–0.091	0.927	1
	B–D	0.365	0.715	1
	C–D	2.556	0.011	0.106
	A–E	–1.826	0.068	0.679
	B–E	–1.369	0.171	1
	C–E	0.822	0.411	1
	D–E	–1.734	0.082	0.828
LA	A–B	–1.279	0.201	1
	A–C	–3.244	0.001	0.012
	B–C	–1.964	0.0495	0.495
	A–D	–1.188	0.235	1
	B–D	0.091	0.927	1
	C–D	2.056	0.040	0.398
	A–E	–2.512	0.012	0.120
	B–E	–1.233	0.217	1
	C–E	0.731	0.465	1
	D–E	–1.325	0.185	1

Multiple comparisons were detected with Dunn's test and p-values were adjusted using the Bonferroni correction; A – HMC (human mesangial cells); B – hypoglycemic group; C – hyperglycemic group; D – mannitol isotonic group; E – rapamycin group; the significance level of the mean difference was 0.05.

no significant difference between the rapamycin group and the hyperglycemic group, the concentrations of Col4, HA and LA were significantly reduced in the rapamycin group.

Discussion

Diabetic nephropathy has become the predominant cause of chronic kidney disease (CKD) in China.[2] Under high glucose conditions, mesangial cells experience abnormal proliferation, resulting in the secretion and deposition of a considerable amount of ECM in the mesangial region.[3] Furthermore, high-glucose conditions also impair autophagy activity in glomerular and renal tubular cells.[4–6] An inhibition of such activity reduces ECM degradation and facilitates DN progression. In many studies on the mechanism of mesangial cells and matrix proliferation, autophagy in mesangial cells has received little consideration.[7]

Autophagy is an intracellular self-degradation process that degrades and recycles misfolded proteins and damaged organelles to maintain cell homeostasis.[8,9] This process is realized through the transport of cytoskeletal microtubule network system, and its molecular mechanism involves essential proteins, such as LAMP1, LAMP2, Rab7, and UVRAG.[10] The mTOR signaling pathway is the main regulatory pathway of autophagy.[11] It contains at least 2 protein complexes with different functions: mTORC 1 and mTORC 2.[12,13] Of these, mTORC 1, that is a rapamycin sensitive protein complex, is one of the main regulatory factors controlling the activity of ULK1 complex. It can modulate autophagy by phosphorylating and dephosphorylating related components within the ULK1 complex, specifically ULK1 and Atg13.

This study aimed to elucidate the impact of high-glucose condition on HMC. The 5-ethynyl-2-deoxyuridine is a nucleoside analogue of thymine (T) and an effective replacement for T in replicating DNA during cell proliferation. The green fluorescence of newly proliferated cells is observed under a fluorescence microscope after staining with Azide 488, with excitation wavelength falling between 495–519 nm. After performing DNA staining with Hoechst 33342, all cells emit blue fluorescence at an excitation wavelength of 346–460 nm, including newly proliferated cells and previously undivided proliferated cells. The results of EdU cell proliferation experiment showed that the number of nuclei and cell proliferation in hyperglycemic group were significantly reduced compared with the other 3 groups (912.0 (860.5–969.5) and 141.0 (130–163.25, respectively), and the proliferation rate was the lowest: 17.5 (13.75–19.75).

The flow cytometry results indicated that the percentage of mesangial cell apoptosis was 16.04% (16.03–16.55%) under high-glucose conditions, surpassing that of the other groups. The high-glucose conditions significantly affected cell survival rates, while the proliferation rate and apoptosis number of cells in the mannitol isotonic group did not differ significantly from those in the HMC group. This finding further demonstrates that high-glucose conditions or its glucose metabolites can impede cell proliferation and promote cell apoptosis, but this effect is unaffected by high

osmotic state. Second, this study confirmed that high-glucose conditions inhibited HMC proliferation and autophagy activity. Autophagy flow detection can determine autophagy state. Changes in autophagy flow are primarily monitored using GFP–RFP–LC3 tandem fluorescent protein labeling, which has sensitivity different to lysosomal acidic microenvironment.[14]

The strength of autophagy can be assessed through red and yellow fluorescence intensity. This study utilized a GFP–RFP–LC3-labeled autophagy flow experiment to demonstrate that the hyperglycemic group had significantly diminished autolysosome count compared to the HMC group, indicating subdued autophagy activity. Previous research has demonstrated that inhibition of autophagy exacerbates oxidative damage in cells. Damaged and aging organelles and macromolecules within cells may not be eliminated in a timely manner, resulting in their accumulation and worsening of cellular damage, aging, and eventual promotion of cell apoptosis. This process could potentially be one of the mechanisms behind the development of DN.[15–17]

LC3 and P62 are proteins commonly used as markers for autophagy, reflecting both its expression and intensity. LC3 is found in 2 forms, LC3-I and LC3-II. Initially, Atg4 cleaves the precursor LC3 to produce LC3-I, which later, under the activation of Atg7, generates its membrane binding form (LC3-II), which locates at autophagosome and autolysosome membranes[18]. The changes in LC3-II protein content can offer insight into the changes in autophagic structures, such as autophagosomes and autolysosome.[19]

P62, a protein that binds to ubiquitin, is essential for autophagy and serves as a selective autophagy receptor that links LC3 to the ubiquitinated substrate targeted for degradation.[20] Western blotting analysis revealed that the expression of LC3-II was significantly lower in the hyperglycemic group compared to the HMC group. Additionally, the LC3-II/LC3-I ratio was reduced, while P62 expression levels were elevated, strongly indicating that hyperglycemia significantly inhibits cellular autophagy activity.

Under high-glucose conditions, inhibition of autophagy decreases ECM degradation, resulting in an ECM synthesis and degradation imbalance. This leads to the accumulation of ECM components such as Col4, HA and LA in the mesangial region of the kidney. Significant increases in Col4, HA and LA contents were observed in the hyperglycemic group compared to other groups.

Rapamycin is a known inducer of autophagy. The study revealed that the addition of rapamycin into the HMC of the hyperglycemic group resulted in a significant increase in the expression of LC3-II compared to other groups. Additionally, the expression of LC3-I and P62 decreased significantly, indicating that rapamycin could activate inhibited autophagy. The levels of Col4, HA and LA of ECM components were reduced in the rapamycin group, as confirmed with ELISA. This indicates that after autophagy was activated, the accumulation of ECM decreased significantly, leading to an improvement in the condition. Nonetheless, no statistical difference was observed between the rapamycin group and the hyperglycemic group, which may be due to the small sample size.

Limitations

The study had a small sample size and an imperfect test grouping. At the outset, the rapamycin group did not undergo cell proliferation or apoptosis tests, and the ELISA test did not yield statistically significant differences in HA, resulting in poor persuasiveness. Additionally, no experiments were conducted to verify rapamycin's autophagy induction effect.

Conclusions

Autophagy activity of glomerular mesangial cells is significantly inhibited under high-glucose conditions, but rapamycin can induce cell autophagy, improve cellular metabolic processes, and reduce mesangial cell proliferation and matrix hyperplasia, thereby inhibiting the progression of DN. This provides a theoretical basis for the clinical application of rapamycin in DN treatment.

Data availability

The datasets generated and/or analyzed during the current study are available from the corresponding author on reasonable request.

Consent for publication

Not applicable.

ORCID iDs

Ya Fu https://orcid.org0000-0002-8861-4271

References

1. Ding Y, Kim JK, Kim SI, et al. TGF-β1 protects against mesangial cell apoptosis via induction of autophagy. *J Biol Chem*. 2010;285(48):37909–37919. doi:10.1074/jbc.M109.093724
2. Zhang L, Long J, Jiang W, et al. Trends in chronic kidney disease in China. *N Engl J Med*. 2016;375(9):905–906. doi:10.1056/NEJMc1602469
3. Wu Z, Yin W, Sun M, Si Y, Wu X, Chen M. BK_{Ca} mediates dysfunction in high glucose-induced mesangial cell injury via TGF-β 1/Smad2/3 signaling pathways. *Int J Endocrinol*. 2020;2020:3260728. doi:10.1155/2020/3260728
4. Kitada M, Ogura Y, Suzuki T, et al. A very-low-protein diet ameliorates advanced diabetic nephropathy through autophagy induction by suppression of the mTORC1 pathway in Wistar fatty rats, an animal model of type 2 diabetes and obesity. *Diabetologia*. 2016;59(6):1307–1317. doi:10.1007/s00125-016-3925-4
5. Takahashi A, Takabatake Y, Kimura T, et al. Autophagy inhibits the accumulation of advanced glycation end products by promoting lysosomal biogenesis and function in the kidney proximal tubules. *Diabetes*. 2017;66(5):1359–1372. doi:10.2337/db16-0397
6. Zhou D, Zhou M, Wang Z, et al. Progranulin alleviates podocyte injury via regulating CAMKK/AMPK-mediated autophagy under diabetic conditions. *J Mol Med*. 2019;97(11):1507–1520. doi:10.1007/s00109-019-01828-3

7. Lin YC, Chang YH, Yang SY, Wu KD, Chu TS. Update of pathophysiology and management of diabetic kidney disease. *J Formos Med Assoc*. 2018;117(8):662–675. doi:10.1016/j.jfma.2018.02.007
8. Cheng Z. The FoxO–autophagy axis in health and disease. *Trends Endocrinol Metab*. 2019;30(9):658–671. doi:10.1016/j.tem.2019.07.009
9. Levine B, Kroemer G. Autophagy in the pathogenesis of disease. *Cell*. 2008;132(1):27–42. doi:10.1016/j.cell.2007.12.018
10. Alessandrini F, Pezzè L, Ciribilli Y. LAMPs: Shedding light on cancer biology. *Semin Oncol*. 2017;44(4):239–253. doi:10.1053/j.seminoncol.2017.10.013
11. Jung CH, Ro SH, Cao J, Otto NM, Kim DH. mTOR regulation of autophagy. *FEBS Lett*. 2010;584(7):1287–1295. doi:10.1016/j.febslet.2010.01.017
12. Jacinto E, Loewith R, Schmidt A, et al. Mammalian TOR complex 2 controls the actin cytoskeleton and is rapamycin insensitive. *Nat Cell Biol*. 2004;6(11):1122–1128. doi:10.1038/ncb1183
13. Loewith R, Jacinto E, Wullschleger S, et al. Two TOR complexes, only one of which is rapamycin-sensitive, have distinct roles in cell growth control. *Mol Cell*. 2002;10(3):457–468. doi:10.1016/S1097-2765(02)00636-6
14. Jin L, Qian Y, Zhou J, et al. Activated CRH receptors inhibit autophagy by repressing conversion of LC3BI to LC3BII. *Cell Signal*. 2019;58:119–130. doi:10.1016/j.cellsig.2019.03.001
15. Mammucari C, Milan G, Romanello V, et al. FoxO3 controls autophagy in skeletal muscle in vivo. *Cell Metab*. 2007;6(6):458–471. doi:10.1016/j.cmet.2007.11.001
16. Xie Z, Klionsky DJ. Autophagosome formation: Core machinery and adaptations. *Nat Cell Biol*. 2007;9(10):1102–1109. doi:10.1038/ncb1007-1102
17. Kondo-Okamoto N, Noda NN, Suzuki SW, et al. Autophagy-related protein 32 acts as autophagic degron and directly initiates mitophagy. *J Biol Chem*. 2012;287(13):10631–10638. doi:10.1074/jbc.M111.299917
18. Maiuri MC, Zalckvar E, Kimchi A, Kroemer G. Self-eating and self-killing: Crosstalk between autophagy and apoptosis. *Nat Rev Mol Cell Biol*. 2007;8(9):741–752. doi:10.1038/nrm2239
19. Kadowaki M, Karim MdR. Cytosolic LC3 ratio as a quantitative index of macroautophagy. *Methods Enzymol*. 2009;452 Pt B:199–213. doi:10.1016/S0076-6879(08)03613-6
20. Boyle KB, Randow F. The role of 'eat-me' signals and autophagy cargo receptors in innate immunity. *Curr Opin Microbiol*. 2013;16(3):339–348. doi:10.1016/j.mib.2013.03.010